The conserved plant PM19 protein functions as an osmosensor and regulator of germination

Ross D. Alexander[1], Pablo Castillejo-Pons[1,2], Omar Alsaif[1,3], Yvonne Stahl[1,4], Madeleine Seale[1,5], Peter C. Morris[1]

[1]Institute of Life and Earth Sciences, School of Energy, Geoscience, Infrastructure and Society, Heriot-Watt University, Riccarton, Edinburgh EH14 4AS
[2]Grupo de Investigación en Biodiversidad, Medio Ambiente y Salud, Universidad de Las Américas, Quito, Ecuador
[3]Saudi Food and Drug Authority, Dammam, Saudi Arabia,
[4]Institute for Developmental Genetics, Heinrich Heine University
[5]University of Oxford, Department of Plant Sciences

r.alexander@hw.ac.uk
pablo.castillejo@udla.edu.ec
yvonne.stahl@hhu.de
maddy.seale@plants.ox.ac.uk
omarabufaris@gmail.com
p.c.morris@hw.ac.uk

Summary

During germination, seeds undergo a dramatic transformation in their water content, which increases from around 10% to 90% within 24 hours. Control of water uptake to the embryo is key to the germination process; failure to imbibe sufficiently can result in seed dormancy. This is strongly affected by environmental factors including drought or salinity and can result in reduced crop establishment and yields. However, the osmosensing mechanisms regulating water uptake in plants have not been described. In this work we show that the highly conserved plant plasma membrane protein AWPM19 is a plant osmosensor, regulating germination under osmotic stress. The AWPM19 protein structurally resembles the yeast osmosensor Sho1, with four transmembrane domains, and the Arabidopsis homologue *PM19L1* will phenotypically complement the *sho1* mutant, showing that it can function as an osmosensor. We find that *PM19L1* is highly

expressed in the seed and seedling during germination and is located in the plasma membrane. Arabidopsis *pm19l1* mutants have reduced germination in the presence of salt or sorbitol. In a striking parallel to osmosensing in yeast, signalling downstream of AWPM19 involves a MAP kinase signal transduction pathway. These results give an indication of how plants are able to sense the availability of water, and has important implications for the study of dormancy, drought and salinity tolerance in crops. Furthermore this provides insight into evolutionary adaptation of plants to a terrestrial environment.

Abiotic stress is a major constraint on agricultural productivity. Drought and salinity are particularly problematic and are exacerbated by anthroprogenic climate change. Many organisms have mechanisms for perceiving and thus adapting to environmental osmotic stress but perception mechanisms in plants have remained elusive [1,2]. In this work we show that the highly conserved plant protein AWPM19 functions as an osmosensor and can regulate germination under osmotic stress. The AWPM19 protein was first identified in the plasma membrane fraction of abscisic acid (ABA) treated wheat cells [3], and subsequently in dormant embryos of barley [4]. AWPM19 has been associated with preharvest sprouting, seed dormancy and drought tolerance in a number of different species [5–8], and expression of AW*PM19* genes is enhanced in rice and Arabidopsis by osmotic stress, drought, salt, ABA and cold [6–8].

PM19L1 is an ancient, highly conserved plasma membrane protein

Analysis of the structure of the protein suggests the presence of four transmembrane domains and a variable C-terminal tail [3,7] (Fig.1B). The amino acid sequences in the four predicted transmembrane domains and in the intracellular loop between helix two and three are highly conserved in all land plants, including liverworts and mosses. This shows the

evolutionary antiquity (approximately 470 million years) of this protein (Fig. 1 A); homologues have not been found in any other organisms including algae (for example the Zygnematophyceae, the closest living relative of land plants [9]). It also implies that the transmembrane domains are not simply structural but have an important and conserved function. In contrast, the predicted extracellular loops and C-terminus are not conserved and are variable in length.

A

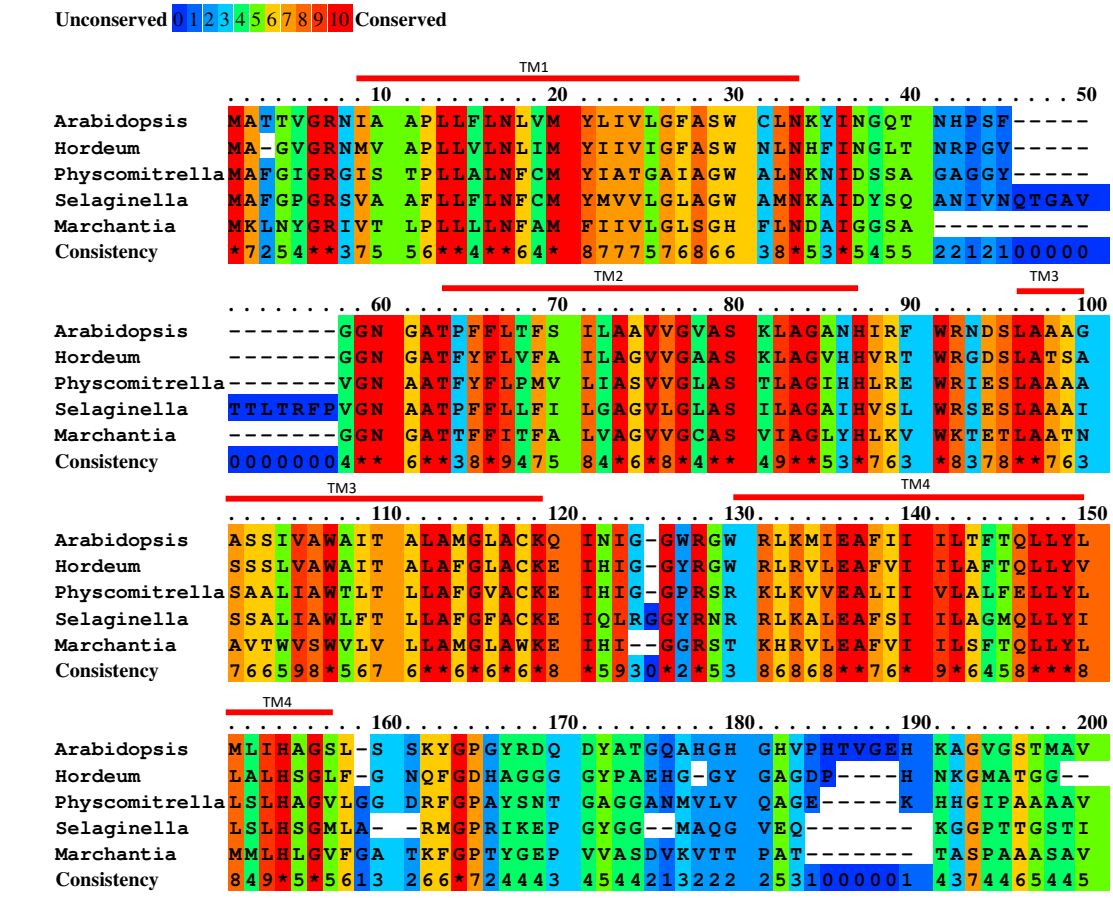

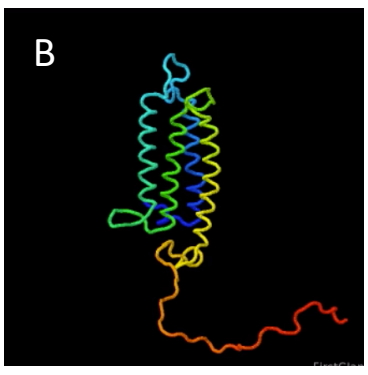

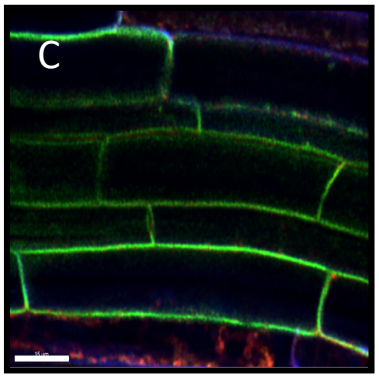

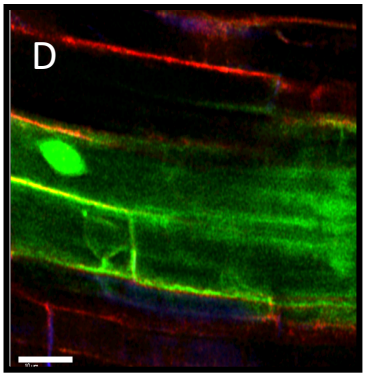

Figure 1. AWPM19 has four transmembrane domains and is highly conserved through terrestrial plant evolution. (A) Alignment analysis of AWPM19 proteins from representative members of all land plants, including bryophytes, vascular plants and seed plants. Red bars indicate position of predicted transmembrane domains. Uniprot sequences *Arabidopsis thaliana* 023029 (the encoded protein from *PM19L1*), *Hordeum vulgare* A0A287T362, *Physcomitrella patens* A9SMF8, *Selaginella moellendorffii* D8S1W8 and *Marchantia polymorpha* A0A2R6WWV5 were aligned using Praline multiple sequence alignment (http://ibi.vu.nl/programs/pralinewww/). (B) Predicted secondary structure of PM19L1 protein carried out with RaptorX and JMol, showing 4 transmembrane alpha helixes and a C-terminal tail (red)(http://raptorx.uchicago.edu/StructurePropertyPred/predict/). (C) Intracellular localisation of PM19L1-GFP (size bar 15 µm) and (D) free GFP (size bar 10 µm) in transgenic Arabidopsis seedling roots as visualised by confocal microscopy. Cells were counterstained with FM4-64 to visualise the plasma membrane and with calcofluor white for the cell wall.

In the model plant *Arabidopsis thaliana*, AWPM19 proteins are encoded for by a 4-member gene family (*PM19L1-4*, [8]). We confirmed plasma membrane localisation of PM19L1 protein [3,6,7] by confocal imaging of cells from transgenic Arabidopsis seedlings expressing free GFP or a PM19L1-GFP fusion driven by the CaMV 35S promoter. PM19L1-GFP exhibited colocalization with FM4-64 at the plasma membrane (Fig. 1 C,D). Transgenic Arabidopsis plants bearing the *PM19L1* promoter sequence fused to the UidA marker gene show high levels of GUS activity in the germinating seedling, but not in vegetative tissues, other than in root tips (Fig.2 A,B). Gene expression of *PM19L1* is highest during seed development and early germination but is also present in all other tissues at lower levels. Expression of the

three other gene family members was not as high as for *PM19L1* in seeds but was seen in all tissues including stems and roots (Fig. 2C, D). Polyethylene glycol (PEG), salts and ABA all upregulated *PM19L1* expression in 14 day-old plants, with a particularly strong effect of PEG, but little effect was seen for the other gene family members (Fig. 2E). An analysis of the phylogenetics for AWPM19 proteins in representatives of all land plant families shows that the Arabidopsis PM19L1 protein is aligned, along with other monocot and eudicot AWPM19 representatives, with the majority of AWPM19 representatives from the bryophytes, whereas PM19L2-4 are on a separate branch and are less tightly aligned to the bryophytes (Fig. SI 1, Table SI 1,2).

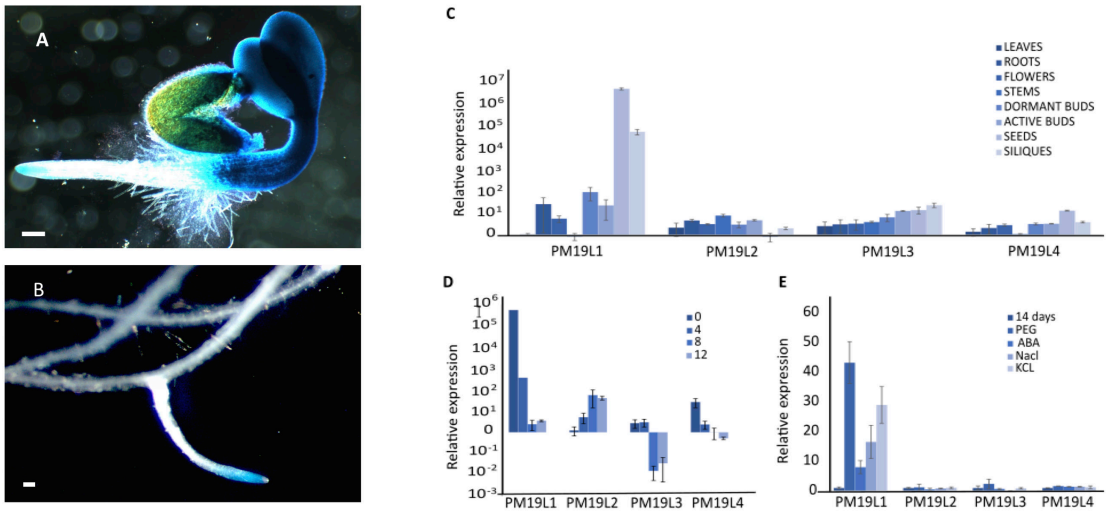

Figure 2. PM19L1 is highly expressed during germination and in root tips. Tissue-specific localisation of PM19L1 gene expression as visualised by staining seedlings bearing the *pPM19L1:UidA* construct for GUS activity, showing high levels of expression in germinating seedlings (A) and in lateral root tips (B) of 14 day old seedlings, bars show 100 µm. Q-PCR analysis of expression patterns for Arabidopsis AWPM19 gene family members in (C) different organs, (D) during germination (bars show days of germination) and (E) in response

to osmotic stresses and ABA; 14 days indicates untreated control plants. Bars show standard deviation.

PM19L1 is associated with osmotic stress during germination

Given the predominantly seed and seedling-specific expression pattern of *PM19L1*, and the induction of *PM19L1* gene expression by osmotica and salts, we suspected that PM19L1 may play a role in germination. We analysed a T-DNA insertion mutant for *PM19L1*, (which did not express detectable mRNA for *PM19L1,* Fig. SI 2), for germination-specific traits. The *pm19l1* mutant was found to be more sensitive than the wildtype to the presence of salts in the germination medium (NaCl, KCl). Similar effects were seen for osmotic stressors such as sorbitol and polyethylene glycol (PEG) (Fig. 3 A, B). Varied results between stressors is not surprising as each of these compounds provides a different type of osmotic stress or toxicity. For example, the greater inhibitory effect of NaCl compared to KCl is characteristic of the cytotoxic effect of sodium. Nevertheless, we observed a consistent trend of decreased germination by salts, sorbitol and PEG that was rescued by complementing the mutant line with *pCaMV 35S*:*PM19L1-GFP.* These data indicate that PM19L1 is involved in the alleviation of osmotic stress. The expression pattern and intracellular location of *PM19L1*, together with the germination phenotype of the *pm19l1* mutant strongly suggests a protein function associated with osmotic stress and water uptake, particularly during germination.

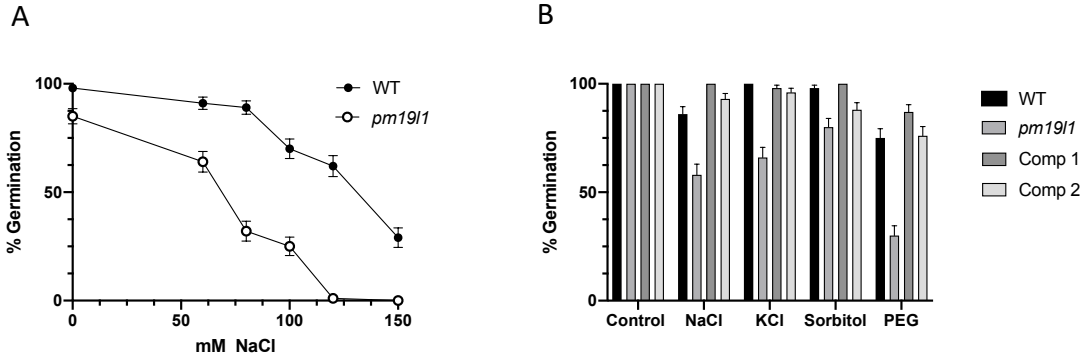

Figure 3. The *pm19l1* mutant is more sensitive to salt and osmotic stress during germination. (A) germination of Columbia wildtype and *pm19l1* mutant seeds on media with varying concentrations of NaCl. (B) Germination of Columbia wildtype, *pm19l1* and two lines complemented with *pCaMV 35S:PM19L1-GFP* on control media and media containing 100 mM NaCl, 100 mM KCl, 200 mM sorbitol and 160 g/l PEG 6000. Bars show standard deviation.

PM19L1 functions as an osmosensor

Plants counter the effects of water and salt stress in many ways, for example, accumulation of osmolytes, exclusion of toxic ions, and reduction of water loss [10]. We explored the possible role of AWPM19 proteins by investigating the physiology of seed germination and by attempting to genetically complement different yeast mutants that have phenotypes associated with salt and osmotic stress, using *PM19L1*. No complementation was seen for the potassium influx transporter mutants *trk1* and *trk2* [11] (Fig. SI 3) nor the sodium efflux mutant *ena1*[12] (Fig. SI 4). Additionally, the levels of sodium and potassium ions in the *pm19l1* mutant did not differ from the wildtype when grown on 60 mM sodium or potassium salts (Fig. SI 5) ruling out the possibility that *AWPM19* genes encode potassium or sodium transporters. Osmolyte accumulation such as proline and soluble sugars in salt-stressed seedlings were no different in wildtype and *pm19l1* seedlings (Fig SI 6 A,B). The yeast glycerol biosynthetic mutant *gdp1*/*gdp2* [13] was also not complemented, indicating that PM19L1 does not have an aquaporin-like function (Fig. SI 7).

However, the yeast *sho1* mutant was fully complemented when *PM19L1* was expressed, permitting growth on up to 500 mM NaCl or sorbitol. Sho1 is an osmosensor that permits growth of yeast on media of high osmolarity by stimulating the Hog1 signalling pathway that controls the accumulation of the osmolyte glycerol [14–16]. The removal of the variable C-terminus of PM19L1 had no impact on the ability of *PM19L1* to complement *sho1* (Fig. 4 A, B). Sho1, like PM19L1, is a four transmembrane domain plasma membrane protein (Fig SI 8) with an extended C terminal, tail but has no protein or DNA sequence homology with the AWPM19 proteins. The ability of an unrelated Arabidopsis four-transmembrane domain plasma membrane protein, tetraspanin, was tested for its ability to complement *sho1*, but it failed to do so (Fig SI 9). This shows that the PM19L1 protein is specific in its ability to function as an osmosensor and suggests a role for PM19L1 in the control of water uptake particularly during germination.

MAP kinase signalling is associated with PM19L1 function

The yeast osmosensing pathway initiates from two osmosensors, the histidine kinase Sln1 and the four transmembrane domain protein Sho1. Downstream from both osmosensors is a kinase signal transduction pathway that is activated under conditions of high osmolarity, with Sln1 activating Ssk2 and Ssk22 (two redundant MAP kinase kinase kinases, MKKK), and the MKKK Ste11 being activated by Sho1. Both activated Ssk2/Ssk22 and Ste11 will in turn activate the MAP kinase kinase (MKK) Pbs2 (which physically interacts with Sho1) and Pbs2 activates the Map kinase Hog1, resulting in the accumulation of glycerol as an osmolyte and the expression of aquaporins to permit water ingress [17,18]. The *pbs2* mutant is compromised by osmotic stress, however growth of *pbs2* on media of high osmolarity is restored by

expression of Arabidopsis MKK2 [19], and Arabidopsis *mkk2* mutants are sensitive to high salt during germination [20].

If Arabidopsis MAP kinase signalling is also involved in plant osmosensing downstream of PM19L1, then co-expression of Arabidopsis *MKK* genes together with *PM19L1* in the yeast *sho1* mutant background would be expected to enhance yeast growth under osmotic stress. This was indeed found to be the case for *AtMKK1, AtMKK2* and *AtMKK3* (all three have all been linked to germination salt stress [20–22]). Co-expression of the Arabidopsis *MKKs* permitted growth on up to 0.75 M sorbitol, whereas PM19L1 on its own only permitted growth on up to 0.5 M sorbitol (Fig. 4C), suggesting that Arabidopsis MKK proteins are associated with downstream signalling from PM19L1, in a similar manner to Pbs2 and Sho1. This association was corroborated by a split ubiquitin analysis in which PM19L1 (and also C-terminally truncated PM19L1) was found to interact with AtMKK1 (weak interaction), AtMKK2 and AtMKK3 (which both showed a stronger interaction (Fig. 4E). MKKs are cytosolic and thus might be expected to interact with the intracellular domains of PM19L1. Site directed mutagenesis of conserved amino acids within the predicted intracellular loop between transmembrane domains 2 and 3 (79 W-G; 80 R-G, 82 D-G) abolished the interaction, however this was not the case (apart for MKK1) when a non-conserved amino acid (81 N-G) in the same loop was changed (Fig. 4D,F). Complementation of *sho1* by *PM19L1* expression was abolished by mutagenesis of the conserved amino acids (Fig SI 10).

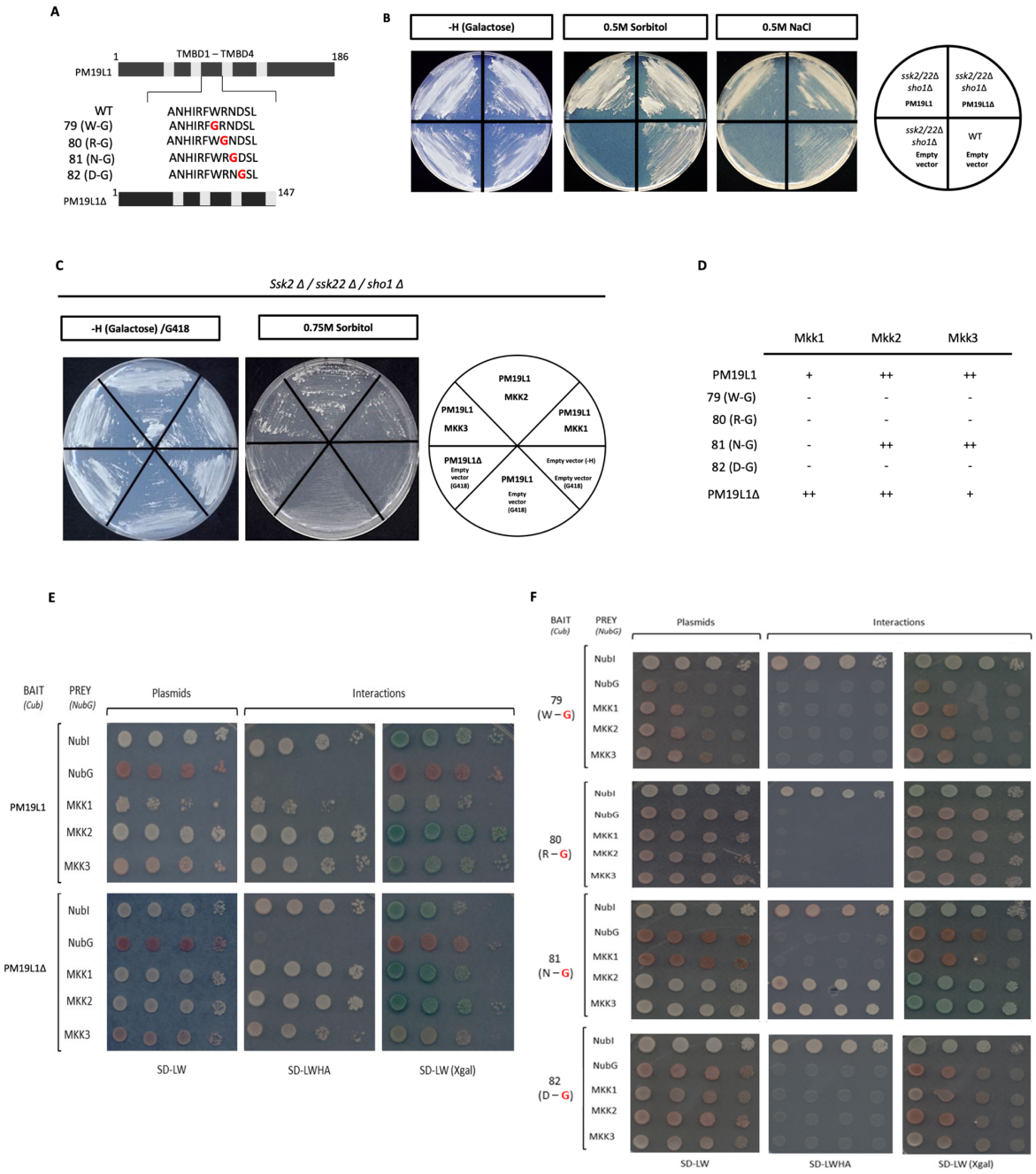

Figure 4. Complementation of the *sho1* mutant in yeast by expression of *PM19L1*. (A) shows the constructs tested, expression of full-length PM19L1 (plasmid pPMRA5), and truncated PM19L1 with the variable C terminus removed (PM19L1Δ)(plasmid pPMRA6). (B) shows growth of wildtype, *skk1/skk2/sho1* mutant, *skk1/skk2/sho1* transformed with *PM19L1*, and with *PM19L1*Δ on basal media, 0.5 M sorbitol and 0.5 M NaCl. (C) co-expression of Arabidopsis MAP kinase kinase (*MKK1*, *MKK2* and *MKK3*) enhances the ability of *PM19L1* to complement *sho1*, resulting in growth on up to 0.75 M sorbitol. (D) is a

summary of split ubiquitin analysis of PM19L1 interactions with Arabidopsis MKK proteins. (E) Split ubiquitin assays showing interactions between PM19L1 or PM19L1Δ with Arabidopsis MKK proteins. NubI is a positive control, NubG a negative control, SD-LW medium selects for presence of bait and prey proteins, SD-LWHA shows growth on media minus histidine and adenine, and SD-LW (Xgal) shows activity of LacZ reporter gene (blue colour). (F) Split ubiquitin assays showing interactions between PM19L1 or PM19L1Δ with Arabidopsis MKK proteins after site-directed mutagenesis to glycine of conserved (79 W-G, 80 R-G and 82 D-G) or non-conserved (81 D-G) amino acids in the intracellular loop of PM19L1.

Discussion

The evidence presented here shows that PM19L1 is an osmoregulator and controls water uptake to the plant, particularly during germination. The exact downstream mechanisms remain to be identified; some have been ruled out here, but other possibilities include regulation of cell wall expansion, or modulation of aquaporin gating. Complementation of yeast osmosensor mutants has been previously used to identify other potential plant osmosensors. The *sln1* mutant (defining the other branch of the Hog1 pathway) is complemented by the Arabidopsis histidine kinase *AHK1* [23,24], and *ahk1* mutants are sensitive to osmolytes during germination [25] although the role of AHK1 in the mature plant has been contested as it is additionally associated with regulation of stomatal density [26]. However, this raises the possibility that AWPM19 and AHK1 fulfil in plant seeds the roles of the two parts of the classic Hog1 osmosensing pathway found in yeast.

The wheat *AWPM19* homologues *PM19-A1* and *PM19-A2* have been identified as QTL candidate genes for preharvest sprouting and dormancy (locus Phs1 on chromosome 4A, [5]),

with expression of these genes being higher in dormant accessions. Additionally, other dormancy QTL genes in both wheat and barley have been identified as being homologues of *MKK3*, the wheat *MKK3*, also mapping to QTL Phs1 [27,28]. This indicates that in cereals, *AWPM19* and *MKK3* both contribute to dormancy and preharvest sprouting by control of water uptake, consistent with a signalling pathway that leads from the osmosensor through a MAP kinase cascade. The rice AWPM19 homologue OSPM1, which is present as multimeric forms in the membrane, has previously been found to facilitate ABA influx in rice[7]. This finding, together with the data presented here, suggests that AWPM19 might function by initially sensing osmotic stress and consequently allowing the influx of ABA to regulate plant responses to stress. Lastly, the evolutionary ancient roots of AWPM19 may represent an important adaptation to terrestrial life for plants in regulating the plant response to osmotic stress.

References

1. Haswell, E. S. & Verslues, P. E. The ongoing search for the molecular basis of plant osmosensing. *J. Gen. Physiol.* **145**, 389-394 (2015).
2. Nongpiur, R. C., Singla-Pareek, S. L. & Pareek, A. The quest for osmosensors in plants. *J. Exp. Bot.* **71**, 595-607 (2020).
3. Koike, M., Takezawa, D., Arakawa, K. & Yoshida, S. Accumulation of 19-kDa plasma membrane polypeptide during induction of freezing tolerance in wheat suspension-cultured cells by abscisic acid. *Plant Cell Physiol.* **38**, 707-716 (1997).
4. Ranford, J. C., Bryce, J. H. & Morris, P. C. PM19, a barley (*Hordeum vulgare* L.) gene encoding a putative plasma membrane protein, is expressed during embryo development and dormancy. *J. Exp. Bot.* **53**, 147-148 (2002).

5. Barrero, J. M. *et al*. Transcriptomic analysis of wheat near-isogenic lines identifies PM19-A1 and A2 as candidates for a major dormancy QTL. *Genome Biol.* **16**, 93 (2015).

6. Chen, H. *et al*. Characterization of OsPM19L1 encoding an AWPM-19-like family protein that is dramatically induced by osmotic stress in rice. *Genet. Mol. Res.* **14**, 11994-12005 (2015).

7. Yao, L. *et al*. The AWPM-19 Family Protein OsPM1 mediates abscisic acid Influx and drought response in rice. *Plant Cell* **30**, 1258-1276 (2018).

8. Barrero, J. M. *et al*. A role for PM19-Like 1 in seed dormancy in Arabidopsis. *Seed Science Research* **29**, 184-196 (2019).

9. Cheng, S. *et al*. Genomes of subaerial Zygnematophyceae provide insights into land plant evolution. *Cell* **179**, 1057-1067.e14 (2019).

10. Gupta, A., Rico-Medina, A. & Caño-Delgado, A. I. The physiology of plant responses to drought. *Science* **368**, 266-269 (2020).

11. Bertl, A. *et al*. Characterization of potassium transport in wild-type and isogenic yeast strains carrying all combinations of trk1, trk2 and tok1 null mutations. *Mol. Microbiol.* **47**, 767-780 (2003).

12. Haro, R., Garciadeblas, B. & Rodríguez-Navarro, A. A novel P-type ATPase from yeast involved in sodium transport. *FEBS Lett.* **291**, 189-191 (1991).

13. Pettersson, N., Hagström, J., Bill, R. M. & Hohmann, S. Expression of heterologous aquaporins for functional analysis in *Saccharomyces cerevisiae*. *Curr. Genet.* **50**, 247-255 (2006).

14. Maeda, T., Takekawa, M. & Saito, H. Activation of yeast PBS2 MAPKK by MAPKKKs or by binding of an SH3-containing osmosensor. *Science* **269**, 554-558 (1995).

15. Saito, H. & Posas, F. Response to hyperosmotic stress. *Genetics* **192**, 289-318 (2012).

16. Tatebayashi, K. *et al*. Osmostress enhances activating phosphorylation of Hog1 MAP kinase by mono-phosphorylated Pbs2 MAP2K. *EMBO J.* **39**, e103444 (2020).

17. O'Rourke, S. M., Herskowitz, I. & O'Shea, E. K. Yeast go the whole HOG for the hyperosmotic response. *Trends Genet.* **18**, 405-412 (2002).

18. Tatebayashi, K. *et al*. Osmosensing and scaffolding functions of the oligomeric four-transmembrane domain osmosensor Sho1. *Nat Commun* **6**, 6975 (2015).

19. Ichimura, K. *et al*. Isolation of ATMEKK1 (a MAP kinase kinase kinase)-interacting proteins and analysis of a MAP kinase cascade in Arabidopsis. *Biochem. Biophys. Res. Commun.* **253**, 532-543 (1998).

20. Teige, M. *et al*. The MKK2 pathway mediates cold and salt stress signaling in Arabidopsis. *Mol. Cell.* **15**, 141-152 (2004).

21. Conroy, C. *et al*. Knockout of AtMKK1 enhances salt tolerance and modifies metabolic activities in Arabidopsis. *Plant Signal. Behav.* **8**, e24206 (2013).

22. Hwa, C.-M. & Yang, X.-C. The AtMKK3 pathway mediates ABA and salt signaling in Arabidopsis. *Acta Physiologiae Plantarum* **30**, 277-286 (2008).

23. Tran, L. S. *et al*. Functional analysis of AHK1/ATHK1 and cytokinin receptor histidine kinases in response to abscisic acid, drought, and salt stress in Arabidopsis. *Proc. Natl. Acad. Sci. U S A* **104**, 20623-20628 (2007).

24. Urao, T. *et al*. A transmembrane hybrid-type histidine kinase in Arabidopsis functions as an osmosensor. *Plant Cell* **11**, 1743-1754 (1999).

25. Wohlbach, D. J., Quirino, B. F. & Sussman, M. R. Analysis of the Arabidopsis histidine kinase ATHK1 reveals a connection between vegetative osmotic stress sensing and seed maturation. *Plant Cell* **20**, 1101-1117 (2008).

26. Kumar, M. N., Jane, W. N. & Verslues, P. E. Role of the putative osmosensor Arabidopsis histidine kinase1 in dehydration avoidance and low-water-potential response. *Plant Physiol.* **161**, 942-953 (2013).

27. Nakamura, S. *et al*. Mitogen-activated protein kinase kinase 3 regulates seed dormancy in barley. *Curr. Biol.* **26**, 775-781 (2016).

28. Torada, A. *et al*. A causal gene for seed dormancy on wheat chromosome 4A encodes a MAP kinase kinase. *Curr. Biol.* **26**, 782-787 (2016).

Methods

Plant material and growth conditions

The Arabidopsis plants used in this study were the wildtype (accession Columbia, Col-0), the homozygous T-DNA insertion mutants *pm19L1 (*line SALK_075435) in the Col-0 background, and transgenic lines bearing the constructs *pCambia1302* and *pCaMV35S:PM19L1-GFP* in both wildtype and *pm19l1* mutant backgrounds, and *pPM19L1:UidA* in the wildtype background.

For agar-grown seedlings, sterilized seeds were sown on half-strength (½) MS medium with additives as indicated in Fig. 3. Plates were placed in a growth chamber with 8/16 h light/dark cycle, with 200 µE m^{-2} s^{-1} white light, 22/20 °C light/dark temperature, and 70% relative humidity. Seeds were harvested from single plants of homozygous lines pot-grown in a mixture of peat (80%) and vermiculite (20%) in a growth chamber with the above-mentioned conditions.

Phylogenetic tree construction

An existing alignment from [7] was used and additional sequences added. The Arabidopsis PM19L1 protein sequence was used for BLAST searches on proteomes available on Phytozome and other sources (see Tables SI 1, 2). No E value cut off was used and all possible sequences were investigated. New protein sequences were added to the existing alignment using mafft-add (MAFFT version 7). The alignment was trimmed to include only regions of the predicted transmembrane domains as illustrated in Fig 1A. This trimmed alignment was then used to construct the phylogenetic tree using PhyML 3.0. The LG protein substitution model, nearest neighbour interchange for tree searching and approximate likelihood ratio (SH-like) branch support settings were used.

Binary plasmid construction and plant transformation

To generate the *pCaMV35S:PM19L1-GFP* lines, the full-length ORF of *PM19L1* (AT1G04560) from cDNA clone *PAP111* (Genbank Z29867)[39] was subjected to site-directed mutagenesis using primers PM19-SDM1 and PM19-SDM2 (Table SI 5) to remove an *Nco*I site from the coding region, and the coding region amplified with primers PM19-NcoI (F) and PM19-Spe1 (R) so as to introduce an *Nco*I site at the encoded N-terminal and a *Spe*I site at the C terminal. This amplicon was cloned into the pCambia1302 vector over *Nco*I and *Spe*I and checked by sequencing to yield the *pCaMV35S:PM19L1-GFP* construct. The construct was transferred into *Agrobacterium tumefaciens* strain EHA105, as was pCambia 1302 as a control, and used to produce transgenic plants by the floral dip method [29]. Transgenic plants were screened for hygromycin resistance, and homozygous T3 generation seeds of 5 independent lines were selected for.

To generate the *pPM19L1:UidA* construct, a 2282 bp fragment was amplified from wildtype Arabidopsis genomic DNA using primers PM19-3 (F) and PM19-SDM2(R) and cloned into pGEM T-Easy. This clone contained 1970 bp of sequence upstream to the *PM19L1* translational start site, and a further 312 bp of coding sequence. A 1257 bp *Eco*RI-*Bgl*II genomic fragment (*Bgl*II is in the 5' untranslated region of *PM19L1*) was excised and cloned into the binary vector pPR97 in front of the *UidA* gene [30], transferred into *Agrobacterium tumefaciens* strain EHA105 and used to produce transgenic plants by the floral dip method [29]. Transgenic plants were screened for kanamycin resistance, and homozygous T3 generation seeds of 10 independent lines were selected for.

Germination assays

Plants were grown in a controlled-environment room at 22 °C constant temperature and a 16-h-light, 8-h-dark photoperiod (200 µE m^{-2} s^{-1}). For germination assays, seeds were sown on 0.8% agar media containing 0.5× MS salts, 10 mM MES pH 5.6, and either osmotica or salts as specified in Fig. 2. Germination was scored for by observing radicle protrusion. 100 seeds were used per assay and analysed using binomial statistics.

For stress treatments, seedlings were grown for 14 days on half-strength (½) MS medium plates in a controlled-environment room at 22 °C constant temperature and a 16-h-light, 8-h-dark photoperiod (200 µE m^{-2} s^{-1}). Seedlings were then sprayed directly with either a 15% w/v solution of PEG 6000, 25 µM ABA, 200 mM NaCl, 200 mM KCl, or distilled water and incubated for 24hrs. They were frozen in liquid nitrogen in pools of 5 seedlings per line in triplicate, ready for RNA extraction and mRNA expression.

Physiological measurements

Measurement of free proline content was carried out according to [31]. Soluble sugars were measured according to [32] using an anthrone reagent. In both cases, triplicate extracts were prepared and measured. Data was analysed for statistical significance by two sided ANOVA and post-hoc Tukey's test for multiple comparisons. Potassium and sodium ion measurements were carried out on aqueous plant extracts using Laqua twin ion-specific electrodes (Horiba Scientific).

Histochemical staining for B-glucuronidase (GUS) assay and imaging

Histochemical GUS staining was carried out on seeds and seedlings of *pPM19L1:UidA* lines, grown on agar plate media as described by [33]. After incubation, the pigments were removed

by repeated washing in 70% (v/v) ethanol. Images of GUS-stained seedlings were recorded with a Leica DFC320 microscope. Imaging of GFP-expressing plants was done using a Leica DMIRE2 confocal microscope with an HCV PL APO CS 40X 1.25 oil immersion lens. GFP excitation wavelength was 488 nm, emission 500-550 nm. FM4-64 excitation wavelength was 561 nm and emission 650-740 nm.

RNA extraction and mRNA expression

Total RNA extraction and cDNA synthesis were performed as described by [34]. Northern blotting was carried out at described by [35]. Plant material was taken from agar-grown seedlings or mature, soil-grown plants as described above. Dormant and active axillary buds were prepared by excising nodal stem segments and placing into microcentrifuge tubes containing liquid half MS for 3 days using a modified protocol described in [36]. Dormant buds were harvested from intact stem segments and active buds harvested after removing the primary shoot apex to activate buds 24 hours previously. Oligonucleotides were designed using Primer3plus [37] (Table SI 5). RT-qPCR was performed with a StepOnePlus™ Real-Time PCR System (Applied Biosystems). Standard cycling conditions were 10 min at 95 °C followed by 40 cycles of 15 s at 95 °C and 1 min at 60 °C; the melting curve profiles were then determined. Reactions were performed in three technical replicas per biological replica and in 3 biological replicas per line and treatment. Expression values were normalized to the Arabidopsis *Actin-2* (*ACT2*, At3g18780) and gene expression values were calculated using the $2^{-\Delta\Delta CT}$ method [38].

Yeast strains and plasmids

All strains and plasmids used for work in the yeast *Saccharomyces cerevisiae are* described in Supplementary Tables SI 3 and SI 4. The ORF from PM19L1 cDNA clone *PAP111* [39] was amplified with primers PM19-3A and PM19-Xba1 to yield a full-length ORF which was cloned into the *Eco*RV site of pBluescript. PM19L1 was re-excised with *Bam*HI and *Xba*I and cloned into pYES2 to yield pPMRA1, which was used to test for complementation of *trk1/trk2* [11] and of *ena1* [12].

To test for complementation of the YSH642 strain (*gdp1/gdp2*) [13], auxotrophic selection over leucine was required, therefore the LEU2 expression cassette from pGAD424 was cloned into the *Apa*I and *Nhe*I sites in the URA3 gene of pYES2 to give pPMRA2, and into pYES2-PM19 to give pPMRA3.

In order to test for complementation of the *sho1* mutant [14], auxotrophic selection over histidine was required, therefore the HIS3 expression cassette from pFA6a-HIS3MX6 was cloned into the *Apa*I and *Nhe*I sites in the URA3 gene of pYES2 to give pPMRA4, and into pYES2-PM19 to give pPMRA5. A shortened version of pPM19L1, which removed the non-conserved C-terminal was created by use of primers PM19-HindIII and Short PM19- XbaI to yield an amplicon encoding a protein of 149 amino acids (PM19L1**Δ**) that was cloned into pPMRA4 to give pPMRA6.

To additionally express Arabidopsis *MKK* genes together with *PM19L1* in the *sho1* mutant, selection over kanamycin was employed, therefore the KAN expression cassette from pFA6a-KANMX6 was cloned into the *Apa*I and *Nhe*I sites in the URA3 gene of pYES2 to give pPMRA7. Subsequently the open reading frames of AtMKK1 (At4g26070), AtMKK2 (At4g29810) and AtMKK3 (At5g40440) were cloned into pPMRA7 to give pPMRA8, pPMRA9 and pPMRA10 respectively. Site directed mutagenesis was used to change specific amino

acids in PM19L1 and these modified versions where introduced into pPMRA4 to give pPMRA11 (79W-G), pPMRA12 (80R-G), and pPMRA13 (82D-G). The Arabidopsis tetraspanin 3 (At3g45600) ORF was amplified using primers TET3-F AND TET3-R and cloned into pPMRA4 to give pPMRA14.

Yeast growth conditions

Yeast cells were grown using standard microbial techniques and media [40]. Media designations are as follows: YPAD is 1% Yeast Extract - 2% Peptone - 2% glucose plus Adenine medium; SDAP is synthetic dextrose arginine phosphate [41]. For YP-Gal, glucose was replaced with 2% galactose. SD is Synthetic Defined dropout (SD-drop-out) medium. Minimal dropout media are designated by the constituent that is omitted (e.g. -leu –trp –his –ade -ura medium media lacks leucine, tryptophan, histidine, adenine and uracil). Recombinant plasmid DNA constructs were introduced using the standard lithium acetate method [42]. Selection and growth of transformants was performed in SD -drop-out lacking the appropriate amino acid or containing the appropriate antibiotic.

Functional complementation of yeast mutants

For complementation analysis all transformed yeast cells were grown in selective media and collected at a density of OD 0.4-0.6. Subsequent fivefold dilutions were made and 5 µl were spotted onto minimal medium plates containing galactose as a carbon source and the indicated osmotica. They were incubated at 30°C (unless stated) for 2–4 days and scanned. Potassium and sodium-dependent phenotypes were analysed using the PLY240 and L5709 strains (Table SI 3) as described in [11] and [12] respectively. For potassium importer assays, WT

(JRY379) and *trk1/2* (PLY240) strains transformed with pYES2 or pPMRA1 were grown on SDAP agar plates (pH 5.8), supplemented with 20 mM KCl. For sodium assays WT (W303-1A) and *ena1* (L5709) strains were transformed with pYES2 or pPMRA1 and grown on SD-ura plates supplemented with different concentrations of NaCl 50 mM to 500 mM. Aquaglyceroporin function was tested by transforming the WT (W303-1A) strain or YSH642 [13] (Table SI 3) with pPMRA2 or pPMRA3 and growing them on SD-L plates supplemented with KCl or sorbitol. The *sho1*Δ, *ssk2*Δ, *ssk22Δ* triple mutant (TM310) [14] was transformed with the pPMRA4 control vector, pPMRA5 and pPMRA6, or mutant variants pPMRA11-13 (Table SI 4). Osmosensitivity of yeast strains was tested by growth on SD-H (Gal) plates with and without different concentrations of NaCl or sorbitol. The *sho1*Δ, *ssk2*Δ, ssk22Δ triple mutant containing pPMRA5 or pPMRA6 was then re-transformed with Arabidopsis MKK1, MKK2 or MKK3 in the yeast vector pPMRA7 containing a kanamycin resistance marker (plasmids pPMRA8-10). These strains were tested by growth on SD-H (Gal) / G418 plates, with and without different concentrations of sorbitol as described in the figure legend (Fig. 4).

Yeast two hybrid screens

Protein-protein interaction analysis was carried out by utilising the split-ubiquitin yeast two-hybrid system [43]. All work was done using strain NMY51 (Dualsystem Biotech, supplemental table SX). NMY51 was first transformed with the pAMBV bait plasmid containing one of 6 different PM19L1 variants (pPMRA15 - 20, Table SI 4). Auto-activation was determined by co-expressing each bait with NubI 'positive' and NubG 'negative' control prey plasmids. Ideally, all transformed strains would be expected to show comparable growth on the

transformation selection medium, but only bait strains containing NubI 'positive' control prey would be expected to grow on the interaction selection medium. Baits containing NubG 'negative' control preys that grow on interaction selection medium are said to be 'self-activating' and are not suitable for screening. All constructs proved suitable for screening. Prey vector pPR3C containing one of the full-length MKK1, MKK2 and MKK3 sequences (pPMRA21-23, Table SI 4) were then co-transformed with strains containing the bait plasmids. Transformants were selected for the presence of both bait and prey plasmids during 3 days of growth at 30°C on SD-trp-leu medium. Positive colonies were transferred to liquid SD-trp-leu medium and grown overnight to an OD of 1.0. Five microliters of different dilutions (1:10, 1:100, 1:1000) were spotted onto transformation selection medium (SD-trp-leu, to ensure that spotted cells are carrying the appropriate plasmids) and onto interaction selection medium (SD-trp-leu-his-ade media and SD-trp-leu -Xgal, to select specifically for cells containing interacting bait–prey pairs). Plates were then incubated for 4 -6 days at 30°C.

29. Clough, S. J. & Bent, A. F. Floral dip: a simplified method for Agrobacterium-mediated transformation of Arabidopsis thaliana. *Plant J.* **16**, 735-743 (1998).

30. Szabados, L., Charrier, B., Kondorosi, A., de Bruijn, F. J. & Ratet, P. New plant promoter and enhancer testing vectors. *Molecular Breeding* **1**, 419-423 (1995).

31. Bates, L. S., Waldren, R. P. & Teare, I. D. Rapid determination of free proline for water stress studies. *Plant and Soil* **39**, 205-207 (1973).

32. Yemm, E. W. & Willis, A. J. The estimation of carbohydrates in plant extracts by anthrone. *Biochem. J.* **57**, 508-514 (1954).

33. Jefferson, R. A., Kavanagh, T. A. & Bevan, M. W. GUS fusions: beta-glucuronidase as a sensitive and versatile gene fusion marker in higher plants. *EMBO J.* **6**, 3901-3907 (1987).

34. Alexander, R. D., Wendelboe-Nelson, C. & Morris, P. C. The barley transcription factor HvMYB1 is a positive regulator of drought tolerance. *Plant Physiology and Biochemistry* **142**, 246-253 (2019).

35. Alzwiy, I. A. & Morris, P. C. A mutation in the Arabidopsis MAP kinase kinase 9 gene results in enhanced seedling stress tolerance. *Plant Sci.* **173**, 302-308 (2007).

36. Seale, M., Bennett, T. & Leyser, O. BRC1 expression regulates bud activation potential but is not necessary or sufficient for bud growth inhibition in Arabidopsis. *Development* **144**, 1661-1673 (2017).

37. Untergasser, A. *et al*. Primer3—new capabilities and interfaces. *Nucleic Acids Res.* **40**, e115-e115 (2012).

38. Schmittgen, T. D. & Livak, K. J. Analyzing real-time PCR data by the comparative C T method. *Nature protocols* **3**, 1101 (2008).

39. Cooke, R. *et al*. Further progress towards a catalogue of all Arabidopsis genes: analysis of a set of 5000 non-redundant ESTs. *Plant J.* **9**, 101-124 (1996).

40. Amberg, D. C., Burke, D. & Strathern, J. N. *Methods in Yeast Genetics* (CSHL Press, 2005).

41. Rodríguez-Navarro, A. & Ramos, J. Dual system for potassium transport in Saccharomyces cerevisiae. *J. Bacteriol.* **159**, 940-945 (1984).

42. Gietz, R. D. & Schiestl, R. H. High-efficiency yeast transformation using the LiAc/SS carrier DNA/PEG method. *Nat Protoc* **2**, 31-34 (2007).

43. Snider, J. *et al*. Detecting interactions with membrane proteins using a membrane two-hybrid assay in yeast. *Nat Protoc* **5**, 1281-1293 (2010).

Acknowledgments

We thank the Saudi Arabian Government for a PhD studentship to Omar Alsaif.

Author Contributions

Ross Alexander carried out yeast complementation, yeast split ubiquitin assays and Q-PCR work, and wrote the manuscript. Pablo Castillejo-Pons carried out mutant phenotype analysis and produced plant transformation constructs, Omar Alsaif carried out mutant phenotype analysis and plant transformations, Yvonne Stahl carried out gene expression studies and helped with protein-protein interaction work, Madeleine Seale carried out gene expression studies and protein phylogeny, Peter Morris conceived the project, designed experiments, carried out mutant phenotype analysis and wrote the manuscript.

Additional Information.

Supplementary information is available for this paper at: XXXXX

The authors declare that all data supporting the findings of this study are available within the paper [and its supplementary information files].

Correspondence and requests for materials should be addressed to PCM.

Supplementary Information

Figure SI 1

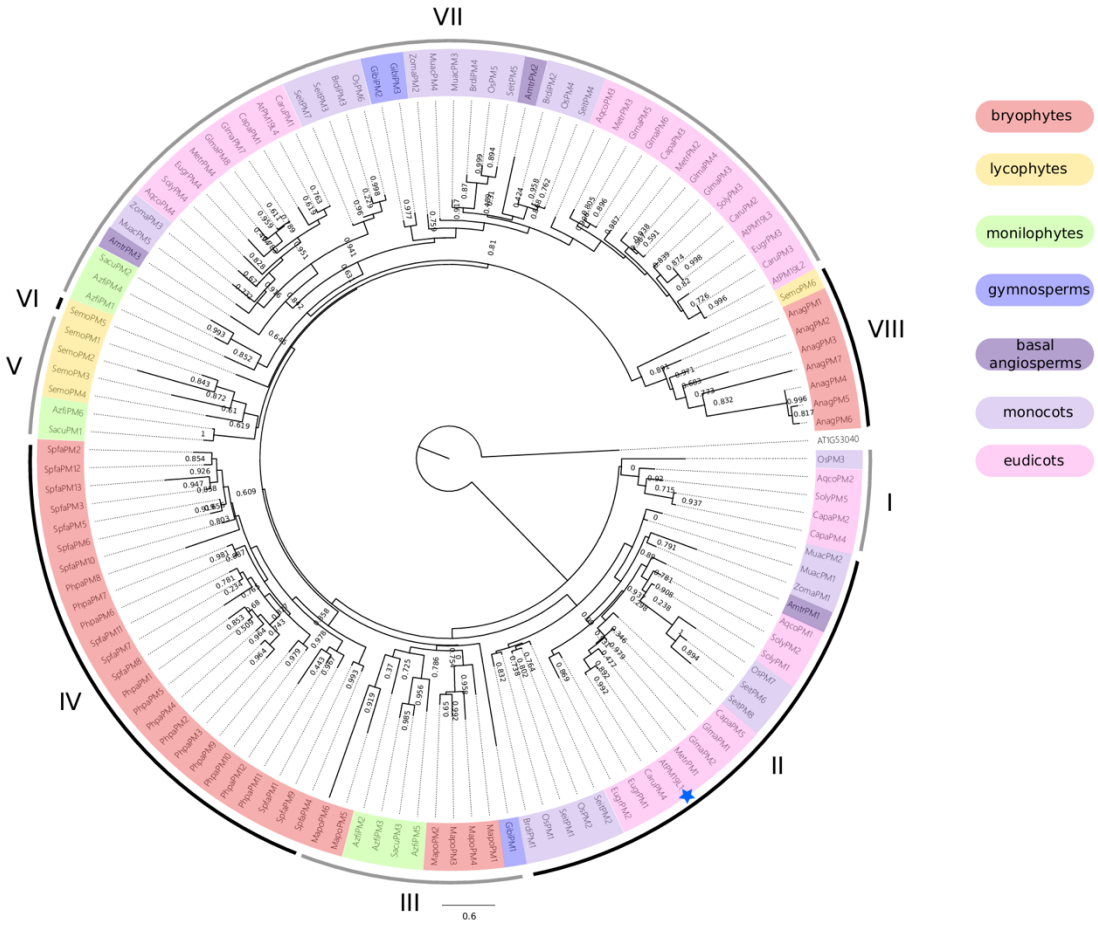

Phylogenetic tree indicating the relationship between AWPM19 family members across land plants. Scale bar indicates mean number of amino acid substitutions per site. Node numbers indicate statistical support for that node configuration according to the approximate likelihood ratio test (aLRT) method. The protein sequence alignment from [7] was used with additional species added here. An Arabidopsis protein, AT1G53040 exhibiting weak sequence similarity to AWPM19 proteins was used as an outgroup to root the tree. Coloured shading illustrates taxonomic divisions and roman numerals indicate monophyletic clades. AtPM19L1 is indicated with the blue star. See table SI 1 for details of species and gene IDs.

The phylogeny demonstrates that the AWPM19 gene family evolved when land plants originated (no similar sequences were found in any algae). Class VII AWPM19 genes appear to be conserved from ferns to angiosperms, while class II, including AtPM19L1 is an angiosperm specific clade. There are also a large number of AWPM19 in bryophytes and some in lycophytes and ferns that have diverged from one another into separate clades and are not generally conserved among seed plants.

Figure SI 2

Northern blot analysis of total RNA isolated from wildtype and *pm19l1* seeds and hybridised with a digoxygenin labled *PM19L1* probe. (A) Ethidium stained RNA, (B) chemiluminescence signal from hybridised probe. There is no detectable signal for PM19L1 in the mutant.

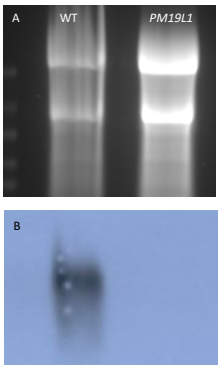

Figure SI 3

Transformation of yeast potassium transporter mutant *trk1/trk2* with Arabidopsis *PM19L1* in plasmid pPMRA1, showing lack of phenotypic complementation on media with low potassium content.

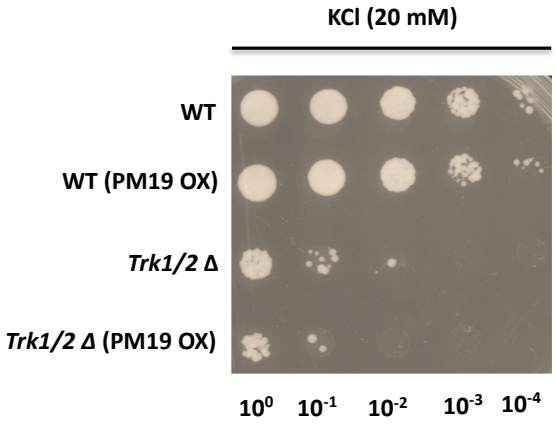

Figure SI 4

Transformation of yeast sodium transporter mutant ena1 with Arabidopsis *PM19L1* in plasmid pPMRA1 showing lack of phenotypic complementation on media with high NaCl.

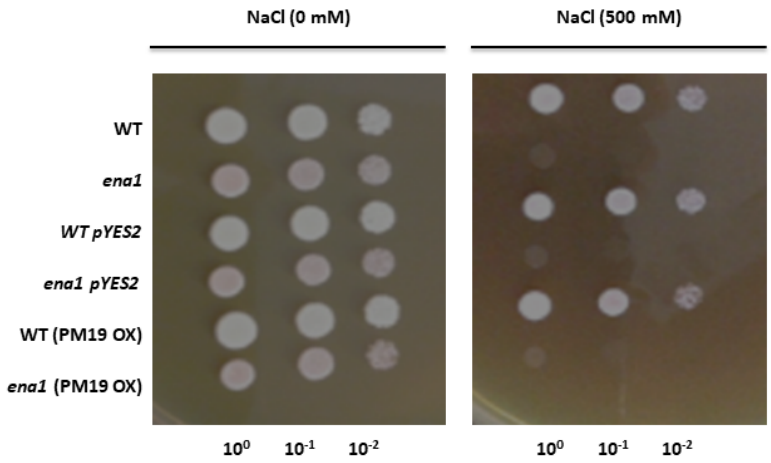

Figure SI 5

Sodium and potassium ion content of wildtype and *pm19l1* mutant seedlings grown for one week on 60 mM NaCl or KCl. Extracts were prepared from triplicate plates. Bars show standard deviation.

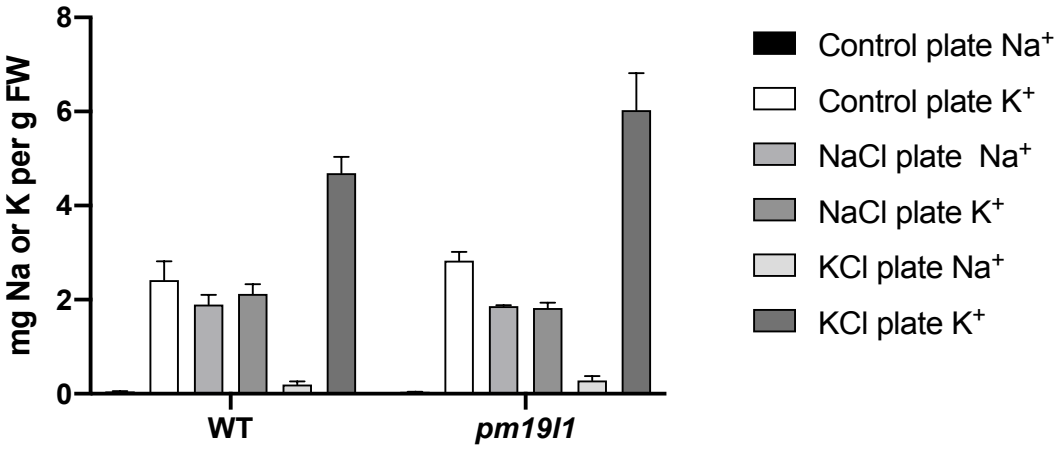

Figure SI 6

(A) Proline and (B) soluble sugars content of wildtype and *pm19l1* mutant seedlings grown for one week on control or 60 mM NaCl containing media. Extracts were prepared from triplicate plates. Bars show standard deviation.

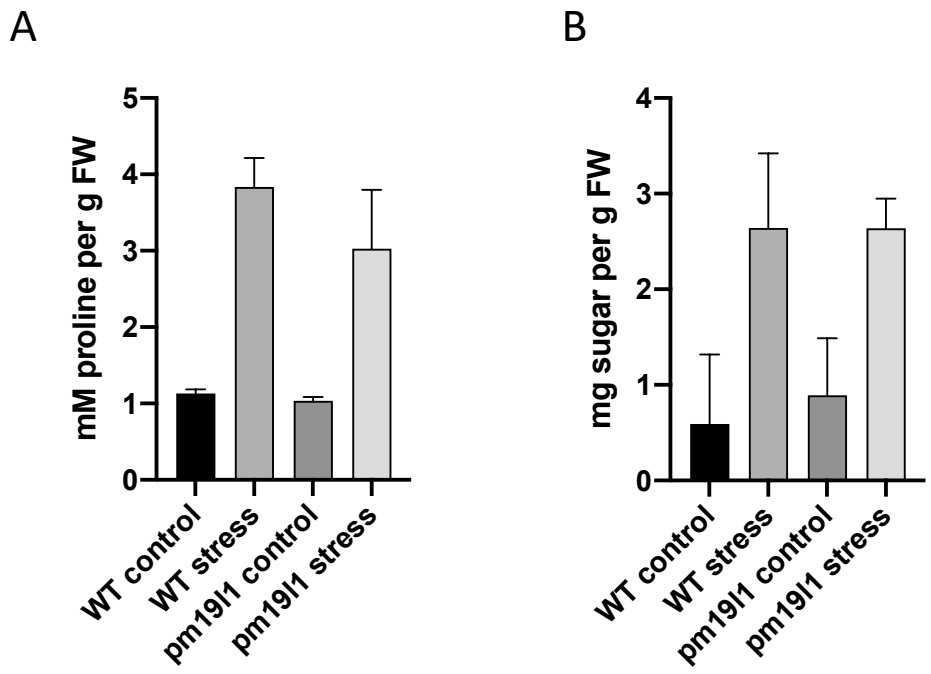

Figure SI 7

Transformation of yeast glycerol biosynthetic mutant *gpd1/gpd2* with Arabidopsis *PM19L1* in plasmid pPMRA3 (PM19 OX), showing lack of phenotypic complementation.

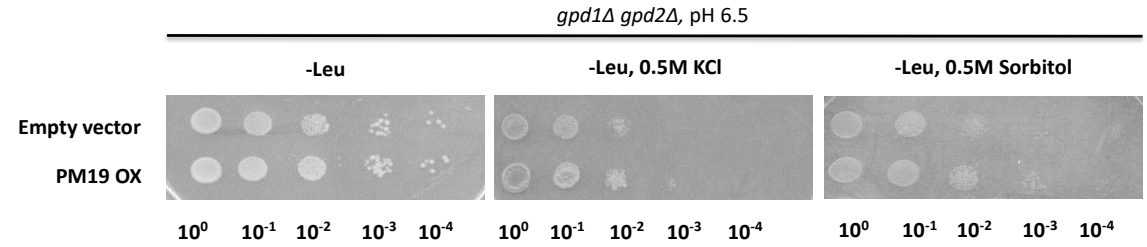

Fig SI 8. Similarity in predicted secondary structure for (A) PM19L1 and (B) Sho1, carried out using Protter (http://wlab.ethz.ch/protter/start/)

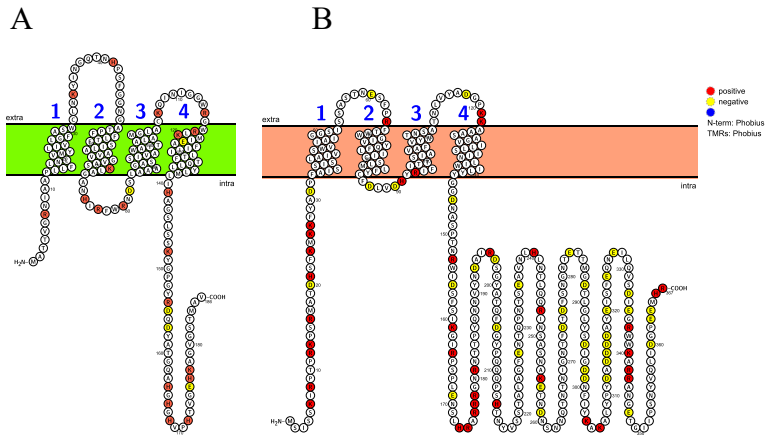

Figure SI 9

Transformation of yeast osmosensing *ssk1/ssk22/sho1* mutant with Arabidopsis tetraspanin (TET-3) and with *PM19L1 (*PM19*)*, showing lack of phenotypic complementation by tetraspanin on media with high osmotic potential.

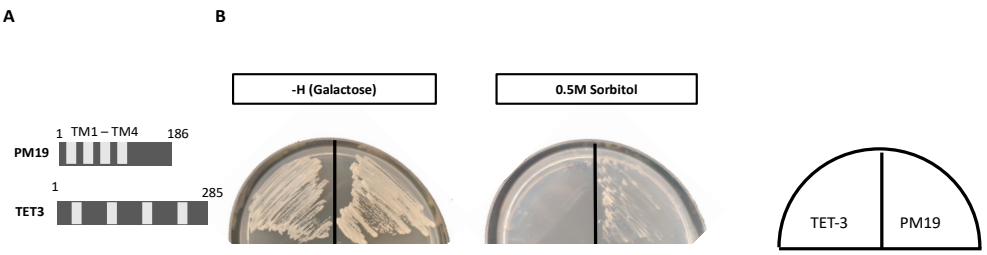

Figure SI 10

Lack of complementation of *sho1* when conserved amino acids in intracellular domain of PM19L1 are modified.

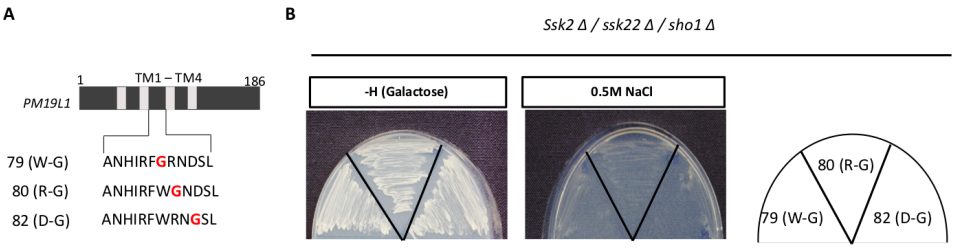

Table SI 1

Number of AWPM19 encoding genes in different plant species, indicating which were added

Species	**Source**	**Genome/proteome version**	**No. proteins found**
Marchantia polymorpha	Phytozome	v3.1	6
Sphagnum fallax	Phytozome	v0.5	13
Zostera marina	Phytozome	v2.2	3
Setaria italica	Phytozome	v2.2	8
Brachypodium distachyon	Phytozome	v3.1	4
Solanum lycopersicum	Phytozome	iTAG2.4	5
Eucalyptus grandis	Phytozome	v2.0	4
Carica papaya	Phytozome	ASGPBv0.4	5
Capsella rubella	Phytozome	v1.0	4
Glycine max	Phytozome	Wm82.a2.v1	8
Medicago truncatula	Phytozome	Mt4.0v1	4
Azolla filiculoides	fernbase	v1.1	6
Salvinia cucullata	fernbase	v1.2	3
Anthoceros agrestis	UniZurich	Oxford	7
Physcomitrium (Physcomitrella) patens	Yao *et al*. 2018		12
Selaginella moellendorffii	Yao *et al*. 2018		6
Ginkgo biloba	Yao *et al*. 2018		3
Amborella trichopoda	Yao *et al*. 2018		3
Aquilegia coerulea	Yao *et al*. 2018		4
Arabidopsis thaliana	Yao *et al*. 2018		4
Musa acuminata	Yao *et al*. 2018		5
Oryza sativa	Yao *et al*. 2018		7

to the existing alignment from Yao *et al*. [7] to create the phylogeny seen in Fig. SI 1.

Table SI 2

Gene IDs for AWPM19-encoding genes added to the existing alignment from Yao *et al*.[7] to create the phylogeny seen in Fig. SI 1.

Species	Gene_ID	Gene_name
Marchantia polymorpha	Mapoly0052s0098.1	MapoPM1
Marchantia polymorpha	Mapoly0022s0083.1	MapoPM2
Marchantia polymorpha	Mapoly0022s0082.1	MapoPM3
Marchantia polymorpha	Mapoly0022s0081.1	MapoPM4
Marchantia polymorpha	Mapoly0044s0120.1	MapoPM5
Marchantia polymorpha	Mapoly0022s0022.1	MapoPM6
Sphagnum fallax	Sphfalx0018s0035.1	SpfaPM1
Sphagnum fallax	Sphfalx0006s0197.1	SpfaPM2
Sphagnum fallax	Sphfalx0176s0017.1	SpfaPM3
Sphagnum fallax	Sphfalx0044s0087.1	SpfaPM4
Sphagnum fallax	Sphfalx0106s0009.1	SpfaPM5
Sphagnum fallax	Sphfalx0027s0209.1	SpfaPM6
Sphagnum fallax	Sphfalx0003s0261.1	SpfaPM7
Sphagnum fallax	Sphfalx0142s0026.1	SpfaPM8
Sphagnum fallax	Sphfalx0205s0031.1	SpfaPM9
Sphagnum fallax	Sphfalx0019s0102.1	SpfaPM10
Sphagnum fallax	Sphfalx0002s0395.1	SpfaPM11
Sphagnum fallax	Sphfalx0006s0346.1	SpfaPM12
Sphagnum fallax	Sphfalx0007s0073.1	SpfaPM13
Zostera marina	Zosma440g00070.1	ZomaPM1
Zostera marina	Zosma88g00500.1	ZomaPM2
Zostera marina	Zosma44g01500.1	ZomaPM3
Setaria italica	Seita.2G115100.1	SeitPM1
Setaria italica	Seita.9G002100.1	SeitPM2
Setaria italica	Seita.3G250100.1	SeitPM3
Setaria italica	Seita.5G284700.1	SeitPM4
Setaria italica	Seita.5G000700.1	SeitPM5
Setaria italica	Seita.9G230400.1	SeitPM6
Setaria italica	Seita.7G125100.1	SeitPM7
Setaria italica	Seita.8G228600.1	SeitPM8
Brachypodium distachyon	Bradi1g00600.1	BrdiPM1
Brachypodium distachyon	Bradi2g47520.2	BrdiPM2
Brachypodium distachyon	Bradi2g25960.1	BrdiPM3
Brachypodium distachyon	Bradi2g08680.1	BrdiPM4
Solanum lycopersicum	Solyc05g053160.2.1	SolyPM1
Solanum lycopersicum	Solyc09g090800.1.1	SolyPM2
Solanum lycopersicum	Solyc02g071310.2.1	SolyPM3
Solanum lycopersicum	Solyc01g080290.2.1	SolyPM4

Solanum lycopersicum	Solyc02g085770.2.1	SolyPM5
Eucalyptus grandis	Eucgr.H00118.1	EugrPM1
Eucalyptus grandis	Eucgr.H02898.1	EugrPM2
Eucalyptus grandis	Eucgr.D00344.1	EugrPM3
Eucalyptus grandis	Eucgr.H03634.1	EugrPM4
Carica papaya	Capa_evm.model.supercontig_16.51	CapaPM1
Carica papaya	Capa_evm.model.supercontig_179.19	CapaPM2
Carica papaya	Capa_evm.model.supercontig_17.171	CapaPM3
Carica papaya	Capa_evm.model.supercontig_179.15	CapaPM4
Carica papaya	Capa_evm.model.supercontig_59.22	CapaPM5
Capsella rubella	Carubv10002111m	CaruPM1
Capsella rubella	Carubv10011510m	CaruPM2
Capsella rubella	Carubv10027229m	CaruPM3
Capsella rubella	Carubv10012389m	CaruPM4
Glycine max	Glyma.20G184600.1	GlmaPM1
Glycine max	Glyma.10G205900.1	GlmaPM2
Glycine max	Glyma.09G085600.1	GlmaPM3
Glycine max	Glyma.15G195600.1	GlmaPM4
Glycine max	Glyma.08G121700.1	GlmaPM5
Glycine max	Glyma.05G164300.1	GlmaPM6
Glycine max	Glyma.07G255100.1	GlmaPM7
Glycine max	Glyma.17G019200.1	GlmaPM8
Medicago truncatula	Medtr1g094035.1	MetrPM1
Medicago truncatula	Medtr2g049340.1	MetrPM2
Medicago truncatula	Medtr6g068860.1	MetrPM3
Medicago truncatula	Medtr4g117600.1	MetrPM4
Azolla filiculoides	Azfi_s0001.g000130	AzfiPM1
Azolla filiculoides	Azfi_s0050.g031077	AzfiPM2
Azolla filiculoides	Azfi_s0185.g056678	AzfiPM3
Azolla filiculoides	Azfi_s0001.g000342	AzfiPM4
Azolla filiculoides	Azfi_s0083.g038896	AzfiPM5
Azolla filiculoides	Azfi_s0003.g007412	AzfiPM6
Salvinia cucullata	Sacu_v1.1_s0019.g007798	SacuPM1
Salvinia cucullata	Sacu_v1.1_s0101.g019776	SacuPM2
Salvinia cucullata	Sacu_v1.1_s0084.g018226	SacuPM3
Anthoceros agrestis	AagrOXF_evm.model.utg000057l.54.1 EVM AagrOXF_evm.TU.utg000057l.54 utg000057l:248554-249384(+)	AnagPM1
Anthoceros agrestis	AagrOXF_evm.model.utg000057l.14.1 EVM AagrOXF_evm.TU.utg000057l.14 utg000057l:74404-75215(-)	AnagPM2
Anthoceros agrestis	AagrOXF_evm.model.utg000004l.46.1 . AagrOXF_evm.TU.utg000004l.46 utg000004l:259567-260346(+)	AnagPM3
Anthoceros agrestis	AagrOXF_evm.model.utg000004l.47.1 . AagrOXF_evm.TU.utg000004l.47 utg000004l:261096-262148(+)	AnagPM4

Anthoceros agrestis	AagrOXF_evm.model.utg000004l.47.2 . AagrOXF_evm.TU.utg000004l.47 utg000004l:261096-262086(+)	AnagPM5
Anthoceros agrestis	AagrOXF_evm.model.utg000004l.47.3 AagrOXF_evm.TU.utg000004l.47 utg000004l:261096-261962(+)	AnagPM6
Anthoceros agrestis	AagrOXF_evm.model.utg000095l.55.1 EVM AagrOXF_evm.TU.utg000095l.55 utg000095l:269706-271270(+)	AnagPM7
Physcomitrium (Physcomitrella) patens	Pp3c4_30620V3.1	PhpaPM1
Physcomitrium (Physcomitrella) patens	Pp3c1_14380V3.1	PhpaPM2
Physcomitrium (Physcomitrella) patens	Pp3c2_25930V3.1	PhpaPM3
Physcomitrium (Physcomitrella) patens	Pp3c11_14870V3.1	PhpaPM4
Physcomitrium (Physcomitrella) patens	Pp3c11_14880V3.1	PhpaPM5
Physcomitrium (Physcomitrella) patens	Pp3c18_17550V3.1	PhpaPM6
Physcomitrium (Physcomitrella) patens	Pp3c4_3450V3.1	PhpaPM7
Physcomitrium (Physcomitrella) patens	Pp3c7_11540V3.1	PhpaPM8
Physcomitrium (Physcomitrella) patens	Pp3c12_25110V3.1	PhpaPM9
Physcomitrium (Physcomitrella) patens	Pp3c4_3440V3.1	PhpaPM10
Physcomitrium (Physcomitrella) patens	Pp3c20_13220V3.1	PhpaPM11
Physcomitrium (Physcomitrella) patens	Pp3c4_21960V3.1	PhpaPM12
Selaginella moellendorffii	Semo439591	SemoPM1
Selaginella moellendorffii	Semo416876	SemoPM2
Selaginella moellendorffii	Semo444324	SemoPM3
Selaginella moellendorffii	Semo37585	SemoPM4
Selaginella moellendorffii	Semo437726	SemoPM5
Selaginella moellendorffii	Semo432371	SemoPM6
Ginkgo biloba	Gb_19410	GibiPM1
Ginkgo biloba	Gb_35411	GibiPM2
Ginkgo biloba	Gb_35398	GibiPM3
Amborella trichopoda	AmTr_v1.0_scaffold00039.123	AmtrPM1
Amborella trichopoda	AmTr_v1.0_scaffold00005.58	AmtrPM2
Amborella trichopoda	AmTr_v1.0_scaffold00025.112	AmtrPM3
Aquilegia coerulea	Aqcoe5G012300.1	AqcoPM1
Aquilegia coerulea	Aqcoe3G398700.1	AqcoPM2
Aquilegia coerulea	Aqcoe1G207600.1	AqcoPM3
Aquilegia coerulea	Aqcoe2G327400.1	AqcoPM4

Arabidopsis thaliana	AT1G04560.1	AtPM19L1
Arabidopsis thaliana	AT5G46530.1	AtPM19L2
Arabidopsis thaliana	AT1G29520.1	AtPM19L3
Arabidopsis thaliana	AT5G18970.1	AtPM19L4
Musa acuminata	GSMUA_Achr8P12720_1	MuacPM1
Musa acuminata	GSMUA_Achr11P02400_1	MuacPM2
Musa acuminata	GSMUA_Achr2P20160_1	MuacPM3
Musa acuminata	GSMUA_Achr4P13350_1	MuacPM4
Musa acuminata	GSMUA_Achr8P06030_1	MuacPM5
Oryza sativa	LOC_Os05g31670.1	OsPM1
Oryza sativa	LOC_Os07g24000.1	OsPM2
Oryza sativa	LOC_Os02g49860.1	OsPM3
Oryza sativa	LOC_Os01g50440.1	OsPM4
Oryza sativa	LOC_Os01g14530.1	OsPM5
Oryza sativa	LOC_Os05g33220.1	OsPM6
Oryza sativa	LOC_Os10g32720.1	OsPM7

Table SI 3: Yeast Strains.

Strain	Description	Source
JRY379	MATa his3, leu2, trp1, ura3, suc2	Prof. Per Ljungdahl, Ludwig institute for Cancer Research, Stockholm, Sweden
PLY240	MATa his3, leu2, trp1, ura3, suc2, trk1Δ51 trk2Δ50::lox-kanMX-lox	Prof. Per Ljungdahl, Ludwig institute for Cancer Research, Stockholm, Sweden
W303-1A	MATa, leu2, ura3, trp1, his3, ade2, can1-100, GAL, SUC2, mal0	Prof. Roberto A. Gaxiola, Arizona State University, USA
YSH642	MATa, leu2-3/112 ura3-1 trp1-1 his3-11/15 ade2-1 can1-100 GAL SUC2, mal0, gpd1Δ::TRP1 gpd2Δ::URA3	Prof. Stefan Hohmann, Chalmers University of Technology Göteborg, Sweden
L5709	MATa, leu2, ura3, trp1, his3, ade2, can1-100, GAL, SUC2, mal0, ena1::HIS3	Prof. Roberto A. Gaxiola (Arizona State University, USA)
TM100	MATa, ura3, leu2, trp1	Prof T. Maeda, Cancer Institute, Tokyo, Japan
TM310	MATa ura3 leu2 trp1 his3 ssk2::URA3 ssk22::LEU2 sho1::TRP1	Prof T. Maeda, Cancer Institute, Tokyo, Japan
NMY51	MATa, his3, trp1, leu2, ade2, LYS2::(lexAop)4-HIS3 ura3::(lexAop)8-lacZ ade2::(lexAop)8-ADE2 GAL)	Dualsystems Biotech AG

Table SI 4: Plasmids used in this work

Plasmid	Features	Use	Source
Complementation assays			
pCambia 1302	CaMV35S:GFP-His	Plant transformation	Prof. Richard Jefferson, Cambia, Australia
pCaMV35S:PM19L1-GFP	pCaMV35S:PM19L1-GFP	Plant transformation	This study
pPR97	UidA	Plant transformation	Prof. P. Ratet, CNRS, France
pPM19L1:UidA	Promoter PM19L1:UidA	Plant transformation	This study
pYES2	2 µm URA3 PGal- CYC1 TT	Expression in yeast	Invitrogen
pPMRA1	PM19L1 in pYES2	Complementation of PLY240 (*trk1/trk2*) RGY85 (*ena1*)	This study
pPMRA2	LEU2 replacement of URA3 in pYES2	Expression in yeast	This study
pPMRA3	PM19L1 in pPMRA2	Complementation of YSH642 (*gdp1/gdp2*)	This study
pPMRA4	HIS3 replacement of URA3 in pYES2	Expression in yeast	This study
pPMRA5	PM19L1 in pPMRA4	Complementation of TM310 (*ssk2/ssk22/sho1*)	This study
pPMRA6	PM19L1**Δ** in pPMRA4	Complementation of TM310 (*ssk2/ssk22/sho1*)	This study
pPMRA7	*Kan(R)* replacement of URA3 in pYES2	Expression in yeast	This study
pPMRA8	MKK1 in pPMRA7	Enhance complementation of TM310	This study

		(*ssk2/ssk22/sho1*)	
pPMRA9	MKK2 in pPMRA6	Enhance complementation of TM310 (*ssk2/ssk22/sho1*)	This study
pPMRA10	MKK3 in pPMRA6	Enhance complementation of TM310 (*ssk2/ssk22/sho1*)	This study
pPMRA11	Mutated PM19L1 (79W-G), in pPMRA5	complementation of TM310 (*ssk2/ssk22/sho1*)	This study
pPMRA12	Mutated PM19L1 (80R-G), in pPMRA5	complementation of TM310 (*ssk2/ssk22/sho1*)	This study
pPMRA13	Mutated PM19L1, (82D-G) in pPMRA5	complementation of TM310 (*ssk2/ssk22/sho1*)	This study
pPMRA14	Tetraspanin in pPMRA4	Complementation of TM310 (*ssk2/ssk22/sho1*)	This study
Split ubiquitin assays			
pOst1-NubI	2 µm, TRP	'Positive' prey vector	Iyer *et al*., 2005
pOst1-NubG	2 µm, TRP	'Negative' prey vector	Iyer *et al.*, 2005
pPR3-C	TRP1 pADH1 - HANubG	Prey vector	Snider *et al.*, 2010
pAMBV	LEU2 pADH1 - Cub-LexA-VP16 tag	Bait vector	Snider *et al.*, 2010
pPMRA15	LEU2 pADH1 - PM19L1 Cub-LexA-VP16 tag	Bait vector	This study
pPMRA16	LEU2 pADH1 - PM19L1**Δ** Cub-LexA-VP16 tag	Bait vector	This study
pPMRA17	LEU2 pADH1 PM19L1**(79W-G)** Cub-LexA-VP16 tag	Bait vector	This study

pPMRA18	LEU2 pADH1-PM19L1**(80R-G)** Cub-LexA-VP16 tag	Bait vector	This study
pPMRA19	LEU2 pADH1-PM19L1**(81N-G)** Cub-LexA-VP16 tag	Bait vector	This study
pPMRA20	LEU2 pADH1-PM19L1**(82D-G)** Cub-LexA-VP16 tag	Bait vector	This study
pPMRA21	TRP1 pADH1 -MKK1-HANubG	Prey vector	This study
pPMRA22	TRP1 pADH1 -MKK2-HANubG	Prey vector	This study
pPMRA23	TRP1 pADH1 -MKK3-HANubG	Prey vector	This study

Table SI 5: DNA primers used in this study.

RT-qPCR	
Primer name	**Primer Sequence(5'3')**
PM19L1_F	GCTTGGTTTTGCAAGTTGGT
PM19L1-R	GAAGAACGGTGTTGCTC
PM19L2_F	TGCTGGAGTTGCTGGAG
PM19L2_R	CAAGCAATAGTGGCGGCAGA
PM19L3_F	TTTTTCAAAAGGCGAAAT
PM19L3_R	CCATCCTCCAATGCCTAGAA

PM19L4_F	CACAAAACTCCCACCTCC
PM19L4_R	AAAGTCTTGTCGCCTTAC
ACT2_F	CTAAGCTCTCAAGATCAAAGGCTTA
ACT2_R	ACTAAAACGCAAAACGAAAGCGGTT
Cloning	
Primer name	**Primer Sequence(5'3')**
PM19-3 F	TAGGGCTTCTACACTGATATG
PM19-SDM 1	CAGCTCTTGCAATGGGGTTGG
PM19-SDM 2	CCAACCCCATTGCAAGAGCTG
PM19-SpeI	AACACTAGTCTTGTGCTC
PM19-NcoI	CAATCCATGGCGACGACA
PM19-3A	CAATTGATGGCGACGACA
PM19-XbaI	CACTCTAGATTCGTTCGTTTGTCA
PM19-HindIII	GCAAGCTTATGGCGACGACAGTGGGA
Short PM19-XbaI	GCTCTAGACTTTGCTGCTGAGTGAACC
TET3-F	TTAAGCTTATGAGAACAAGCAACCAT
TET3-R	TTGAATTCTCAAAGATGGAAATGACT

Site directed mutagenesis	
PM19-SDM 1	CAGCTCTTGCAATGGGGTTGG
PM19-SDM 2	CCAACCCCATTGCAAGAGCTG
79 W-G F	AATCATATTAGGTTTGGGAGGAATGATAGTTTA
79 W-G R	TAAACTATCATTCCTCCCAAACCTAATATGATT
80 R-G F	CATATTAGGTTTTGGGGGAATGATAGTTTAGCC
80 R-G R	GGCTAAACTATCATTCCCCCAAAACCTAATATG
82 D-G F	AGGTTTTGGAGGAATGGTAGTTTAGCCGCTGCT
82 D-G R	AGCAGCGGCTAAACTACCATTCCTCCAAAACCT
81 N-G F	AGGTTTTGGAGGGGTGATAGTTTAGCCGCTGCT
81 N-G R	AGCAGCGGCTAAACTATCACCCCTCCAAAACCT